International Journal of Automotive Technology, Vol. 20, No. 5, pp. 933–942 (2019)
DOI 10.1007/s12239–019–0087–7

pISSN 1229–9138/ eISSN 1976–3832

NUMERICAL STUDY OF THE COMBUSTION CHARACTERISTICS IN A SYNGAS-DIESEL DUAL-FUEL ENGINE UNDER LEAN CONDITION

Abubaker Ahmed Mohammed Mohammed Ali[1)], Kabbir Ali[1)], Changup Kim[2)], Yonggyu Lee[2)], Seungmook Oh[2)] and Kiseong Kim[1)*]

[1)]Department of Mechanical Design Engineering, Chonnam National University, Jeonnam 59626, Korea
[2)]Green Power Laboratory, Korea Institute of Machinery & Materials, 156 Gajeongbuk-ro, Yuseong-gu, Daejeon 34103, Korea

(Received 4 January 2019; Revised 22 February 2019; Accepted 25 February 2019)

ABSTRACT–The aim of this study was to investigate the combustion characteristics of a syngas-diesel dual fuel engine operates in very lean fuel-air mixture conditions. 3D CFD simulation combined with chemical kinetics were used for analysis. The main parameter for this study was the hydrogen content in the syngas. To simulate the combustion for the dual fuel engine, a new dual-fuel chemical kinetics set was used that was constituted by merging the two chemical kinetics sets: n-heptane (173 species), and Gri-mech 3.0 (53 species) for natural gas. The calculation results were in good agreements with the experimental results. Most of the diesel fuel burned as premixed combustion mode. When the hydrogen concentration was high, as in syngas45, most of the syngas in the piston bowl and squish region, except near the cylinder wall, was combusted in the vicinity of TDC; but when hydrogen concentration was low, as in syngas25, flame propagation to the central region of the piston was delayed, which led to an increase of time loss and unburned syngas emission. Due to the strong reverse squish flow, the syngas composition did not affect the flame arrival time at the cylinder wall through the squish area by much.

KEY WORDS : LSLB dual-fuel engine, CFD simulation, Chemical kinetics, Lean combustion, Syngas, Hydrogen content

NOMENCLATURE

ABDC : after bottom dead center
ATDC : after top dead center
BBDC : before bottom dead center
BTDC : before top dead center
CFD : computational fluid dynamics
CO : carbon monoxide
DCC : dynamic cell clustering
DIT : diesel injection timing
d_n : nozzle diameter
EVO : exhaust valve opening
HRR : heat release rate
IMEP : indicated mean effective pressure
IVC : intake valve closing
LSLB : low calorific value syngas lean burn
NOx : oxides of nitrogen
rpm : revolution per minute
TDC : top dead center
θ_{dur} : injection duration
θ_{SOI} : start of injection

1. INTRODUCTION

In recent decades, the demand for alternative fuels has rapidly been increasing, due to the need for the uniform use of various fuels, reduction of air pollution, and rising fuel prices. Coal is the most abundant fossil fuel on the planet, and technology to produce syngas through coal gasification has been developed to reduce air pollution. Efforts are being made to use this syngas as fuel for the reciprocating engines of electric power plants. Syngas produced by coal gasification is composed mainly of combustible gases such as carbon monoxide, hydrogen, and methane, and incombustible gases, such as nitrogen and carbon dioxide. Syngas can be converted to Coal to Liquid (CTL) through the Fisher-Tropsch synthesis process, and off-gas emanates from the process. The off-gas contains significant amounts of nitrogen and carbon dioxide, which are incombustible gases, and the calorific value is very low. This off-gas mixed with syngas can also be used as a fuel for the reciprocating engines of power plants. Syngas-fueled engines are used primarily as dual-fuel engines to facilitate combustion. This is because methane, carbon monoxide and hydrogen, which are the main components of syngas, have a high auto-ignition temperature; hence the difficulty in compression ignition, and therefore the requirement for ignition seeds, such as diesel fuel. Because of the high anti-knock behavior of the syngas, dual-fuel engines using these fuels can achieve high thermal efficiency by enabling high compression ratio under lean mixture conditions.

A number of researchers have conducted studies on

**Corresponding author*. e-mail: sngkim@jnu.ac.kr

syngas-diesel dual-fuel engines, and have reported low NOx emissions and high thermal efficiency (Karim and Moore, 1990; Karim and Wierzba, 1992; Bilcan, 2003; McMillian and Lawson, 2006; Christodoulou and Megaritis, 2014). The effects of several engine-operating parameters, such as injection pressure, load, engine speed, EGR rate on the emission, and the performance of dual-fuel engines, have been investigated (Karim, 1991; Tomita, 2007; Jamrozik *et al*., 2018). Also, combustion characteristics have been surveyed for dual-fuel engines with various gaseous fuels, including natural gas, biogas, and syngas with different constituents (Bilcan *et al*., 2001; Selim, 2005; Sahoo *et al*., 2009; Lata *et al*., 2011; Elnajjar *et al*., 2013). Most previous studies on dual-fuel engines have been conducted for gas fuels with high calorific value. In this study, a very small amount of diesel was injected, and functioned only as an ignition source. The syngas of this study is in real terms the off-gas/syngas mixture, so it has a very low calorific value, and because it is a power generation engine, lean mixture operation is essential to obtain high thermal efficiency.

In such a Low calorific value Syngas Lean Burn (LSLB) dual-fuel engine, problems due to the overly lean mixture and low combustion temperature may occur, such as flame quenching and much emission of unburned syngas. Hence, an appropriate dual-fuel combustion tactic is necessary.

In order to alleviate the problems of the LSLB dual-fuel engine, it is essential to increase the diesel injection quantity to spread the diesel fuel widely in the combustion chamber by using high injection speed; in that way, auto-ignition can be triggered in a wide range of area. Then the flame propagation distances to the remaining region of the combustion chamber can be shortened. Increasing the hydrogen content of syngas can also help, because the laminar flame speed of hydrogen is about 6 times faster than that of methane, which can increase the syngas burning rate. The syngas with the higher H_2 content showed higher maximum pressure and heat release rates, and resulted in higher thermal efficiency and lower HC and CO emissions (Azimov *et al*., 2012; Talibi *et al*., 2014).

In order to understand the combustion characteristics of the LSLB dual-fuel engine, it is necessary to conduct 3D CFD analysis on very complicated phenomena, such as flow, spray, combustion, and pollutants formation in the combustion chamber of the engine, in addition to the engine test. An appropriate chemical kinetics set of the fuel burning process is crucial to improve the accuracy of engine combustion analysis.

Many researchers have developed a chemical kinetics mechanism to simulate syngas and diesel combustion, respectively. Yetter *et al*. (1991) developed a comprehensive chemical kinetics mechanism for CO and H_2, which are the main combustible species in syngas. Saxena and Williams (2006) used KIVA-3V code combined with a chemical kinetics set that consists of 43 species and 173 reactions for simulating the dual fuel engine at part load conditions. Maghbouli *et al*. (2013) used 3D-CFD model combined with a chemical kinetics set that includes 42 species and 57 reactions to analyze the combustion phenomena in the diesel and dual fuel engine.

Since in this study, the LSLB dual-fuel engine has similar diesel and syngas mass ratios, it is appropriate to use a combination of chemical kinetics sets, which are proven to be suitable for diesel fuel and syngas, respectively, for the combustion analysis of syngas-diesel dual-fuel engines. Therefore, it is necessary to construct a combined chemical kinetics set.

The objective of this work is to investigate the combustion characteristics of a syngas-diesel dual fuel engine, which operates in lean fuel-air mixture conditions for power plant usages. Investigations were conducted using 3D CFD simulation including combustion chemical kinetics, and the calculated results were compared with the experimental ones. The main parameter for this study was the hydrogen content in the syngas, since it has much effect on the flame propagation speed.

The different points in the current work from the other related dual fuel engine works are that the amount of diesel is significant; about 20 % of the full load and the engine operates in the excessively lean syngas mixture; up to ϕ syngas ~ 0.235 in IMEP 5 bar.

In these excessively lean syngas mixture conditions, to compensate the slow flame speed, a significant amount of diesel fuel should be injected, which can result in spreading ignition seeds in wide regions in a very short time.

2. ENGINE SPECIFICATIONS AND OPERATING CONDITIONS

A 6-cylinder diesel engine for power plants was modified as a single cylinder syngas-diesel dual-fuel engine. Tables

Table 1. Engine specifications.

Bore	123 mm		
Stroke	155 mm		
Compression ratio	17.1		
Speed	1800 rpm		
Intake valve	18° BTDC/34° ABDC		
Exhaust valve	46° BBDC/18° ATDC		
Injection pump	Zexel in-line "P"		
Injection nozzle	5 holes, d_n = 0.37 mm		
Needle opening pressure	1st: 160 bar, 2nd: 220 bar		
Injection timing	6G	θ_{SOI}	13.91° BTDC
		θ_{dur}	5.2°
	8G	θ_{SOI}	21.40° BTDC
		θ_{dur}	5.2°

Table 2. Syngas composition.

Syngas 25	H_2: 25 %, CO_2: 10 %, CO: 15 %, N_2: 50 %
Syngas 35	H_2: 35 %, CO_2: 10 %, CO: 15 %, N_2: 40 %
Syngas 45	H_2: 45 %, CO_2: 10 %, CO: 15 %, N_2: 30 %

Table 3. Engine operating conditions.

Diesel fuel mode		
IMEP (bar)	Inj. timing	Diesel flow rate (g/s)
1.5	6G	0.276

Dual fuel mode (Diesel + Syngas)							
Syngas Compos.	IMEP bar	Inj. timing	Flow rate		Equivalence ratio (ϕ)		
			Syngas (L/min)	Diesel (g/s)	Syngas only	Diesel only	Over-all
Syngas 25	5	8G	287	0.292	0.240	0.173	0.209
Syngas 35	5	6G	229	0.277	0.243	0.164	0.195
		8G	225	0.29	0.235	0.171	0.202
Syngas 45	5	8G	187	0.298	0.235	0.176	0.202

1 ~ 3 list the details of the engine specifications and operating conditions, respectively used in this study. The engine was equipped with an in-line pump injection system, which has a two-spring injector with 5-hole nozzle. The piston bowl of the engine has a toroidal shape, and its center is shifted by 5.9 mm from the cylinder axis. The injector is mounted at an angle of 8 degrees to the cylinder axis. Due to the offset of the piston bowl and the tilting of the injector from the cylinder axis, the combustion chamber, including diesel spray, is slightly asymmetric, but each nozzle hole of the injector has a different injection angle targeted at similar heights in the side wall of the piston bowl, so the resulting combustion pattern of each hole might be similar. Therefore, in CFD calculations, the combustion chamber was assumed as axisymmetric. Engine experiments were conducted at the Korea Institute of Machinery and Materials (KIMM).

2.1. Initial Conditions for the Simulation

For engine simulations from IVC to EVO, initial conditions of the various parameters in the combustion chamber, such as the gas compositions, temperature, pressure, and the flow variables: the swirl ratio and turbulence intensity, are required. In the IVC, the gas composition and the mixture temperature in the combustion chamber are deduced from various physical quantities, including the amount of air, fuels, and combustion chamber pressure measured during the engine test. The swirl ratio of the engine was calculated as 1.58 by 3D flow analysis of the intake process with ANSYS Forte, which is very similar to the value in Ref. (Claudio *et al*., 2015).

2.2. Injection Parameters

In the LSLB dual-fuel engine, the injection parameters have a significant effect on the spray combustion and subsequent flame propagation into syngas mixture regions. Therefore, in order to simulate the combustion process in the combustion chamber well, the injection parameters must reflect the real values of the engine. Injection timing is determined by measuring the signal of the pressure sensor installed on the fuel line in contact with the injector and setting the start of injection (θ_{SOI}) and injection duration (θ_{dur}). When the needle is opened, it can be seen that the pressure suddenly drops twice, because a two-spring injector with needle opening pressures (1st: 160 bar and 2nd: 220 bar is used. Experiments and calculations were performed at two injection-timing conditions, denoted as 6G and 8G. The diesel injection rate is 0.277 g/s ~ 0.298 g/s at engine speed of 1,800 rpm, similar to IMEP 1.5 bar load condition in diesel mode operation. The spray angle and Sauter Mean Diameter (SMD) were estimated using the empirical formula of Hiroyasu and Masataka (1990).

2.3. CFD Models

ANSYS FORTÉ code was used for the 3D CFD simulations. To decrease computing time, the combustion chamber was considered as axi-symmetric, so the 72° sector mesh with periodic boundary conditions was used to model it, since the injector has five nozzle holes.

The effect of the mesh size on the calculation results was investigated, and the standard mesh as shown in Figure 1 was selected. Because there is no meaningful difference in the calculated combustion chamber pressure between the standard mesh and the fine mesh as shown in Figure 2. Calculations were performed from IVC to EVO.

RANS RNG K-epsilon model was used for turbulence, and the Abani *et al*. (2008) gas-jet model was used to decrease grid reliance for the spray breakup model by concretely modeling the gas entrainment into the spray jet. However, it is reported that the gas-jet model has some weakness in reflecting swirl effects. KH-RT models (Beale

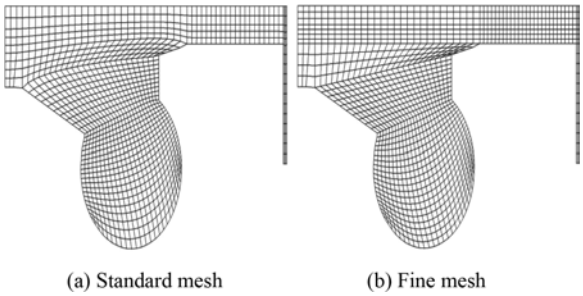

Figure 1. Computed mesh.

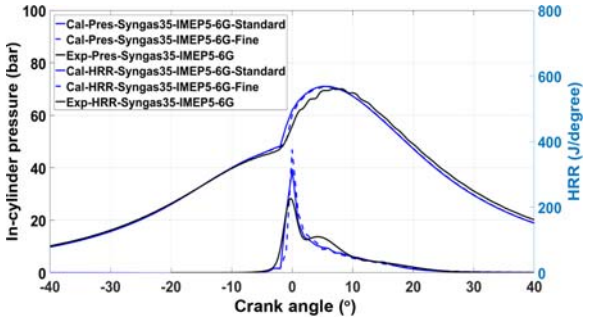

Figure 2. Computed in-cylinder pressure and HRR results of two types of mesh.

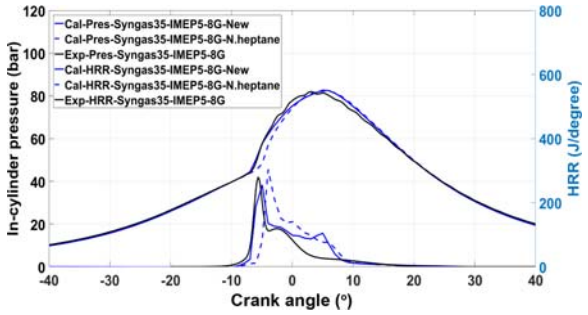

Figure 3. Comparison of the experimental and calculated in-cylinder pressure and HRR of dual-fuel mode using the new chemical kinetics set and n-heptane chemical kinetics set.

and Reitz, 1999; Wang *et al*., 2010) were used for spray drops-splitting. An operator-splitting method was used to solve the chemical kinetics equations for all species in CFD simulation. Some chemistry solution methods were used to enhance the simulation speed in FORTE, like built-in sparse-matrix, and dynamic cell clustering (DCC) (Liang *et al*., 2009).

2.4. Chemical Kinetics

In order to improve the accuracy of the combustion process of the LSLB dual-fuel engine, a chemical kinetics set suitable for the combustion of diesel and syngas fuels should be reflected.

The n-heptane chemical kinetic set and the Gri-mech 3.0 (Smith *et al*., 2018) chemical kinetic set were synthesized to calculate the diesel and syngas combustion reactions, because n-heptane has a comparable Cetane number and combustion characteristics to diesel fuel, and is accepted as surrogate fuel for diesel in both experimental and numerical study (Yang *et al*., 2014; Maroteaux, 2017; Li *et al*., 2018; Liang *et al*., 2018). As n-heptane chemical kinetics set, Diesel_ 1comp_173sp composed of 173 species and 1,100 reactions was used, which captures the pathways necessary for both high-temperature and low-temperature reactions, including the intermediate negative-temperature coefficient regime. The Diesel_ 1comp_173sp chemical kinetics set has been used for a wide variety of temperature, pressure, and equivalence ratio conditions, and has provided accurate results (Ansys Forte, 2017; Stylianidis *et al*., 2017; Curran, 2018). The Gri-mech 3.0 (Smith *et al*., 2018) chemical kinetics set was used for syngas, because syngas in the present work consists of H_2, CO, N_2, and CO_2. Generally, Gri-mech 3.0 composed of 53 species and 325 reactions is a well-established mechanism for modeling natural gas combustion.

A new dual-fuel chemical kinetics set was constituted by merging the two chemical kinetics sets: Diesel_ 1comp_173sp and Gri-mech 3.0.

Figure 3 shows the experimental and calculation results by applying two different chemical kinetics sets: Diesel_1comp_173sp, and the new chemical kinetics set for dual-fuel mode engine operation. The calculated pressure and heat release rate were well matched the experimental results for the case of the new chemical kinetic set, but rather large difference exists for Diesel_1comp_173sp. The new chemical kinetic set successfully caught the auto-ignition points and combustion durations. Thus, the new chemical kinetic set was used for all cases of the later calculation.

3. RESULTS AND DISCUSSION

3.1. General Combustion Characteristics of the LSLB Dual-fuel Engine

A key feature of the LSLB dual-fuel engine is that syngas has a low calorific value, and burns in excessively lean mixture conditions. Table 3 shows that the syngas only equivalence ratio is 0.235, which is low enough to approximate the lower flammability limit. To compensate the two obstacles in the LSLB dual-fuel engine, the diesel injection amount should be much higher than that of a conventional dual-fuel engine. In this study, it reaches about 20 % of that of the full load. This amount of diesel injection through the five nozzle holes is effective in shortening the flame propagation distance in the syngas mixture by spreading the ignition seed of diesel into the combustion chamber deeply and widely in a short time.

Figure 4 shows the combustion chamber pressure and the HRR results of the experiments and calculations when operating in dual-mode and diesel-only mode, while Figure 5 shows the concentrations of n-heptane, CH and OH radicals during combustion, in order to investigate the combustion pattern of the LSLB dual-fuel engine. The ignition timing and the pattern of the early stage of the combustion with the rapid pressure rise in the dual-fuel mode are almost the same as those in the diesel-only mode, which can be characterized as the phenomena in the premixed combustion phase in the four stages of diesel spray combustion, i.e., ignition delay, premixed combustion, mixing-controlled combustion, and late combustion. In the premixed combustion phase, a large portion of fuel that has been evaporated from droplets and

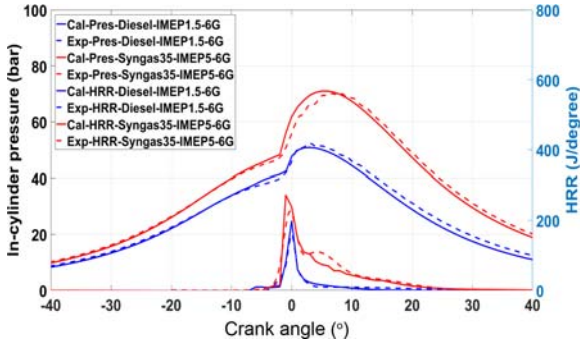

Figure 4. Comparison of the experimental and calculated in-cylinder pressure and HRR of diesel only mode and dual-mode.

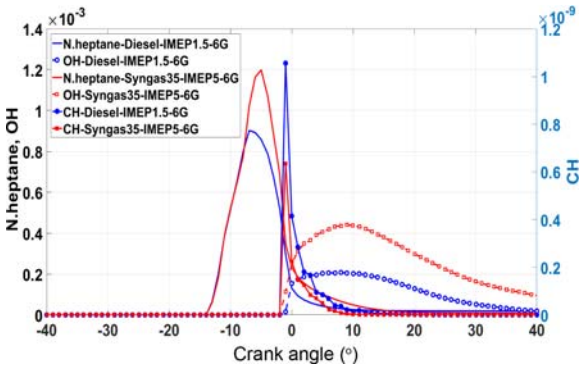

Figure 5. Calculation results of the molar fraction of n-Heptane, OH, and CH of diesel only mode and dual-fuel Mode.

mixed with air during the ignition delay period burns rapidly, and causes abrupt increase of the pressure in the combustion chamber. The auto-ignition of the LSLB dual-fuel engine depends solely on diesel, because the auto-ignition temperatures of hydrogen and carbon monoxide are as high as 585 °C and 605 °C, respectively, at atmospheric pressure. The HRR pattern, which occurs during the mixing controlled combustion phase of a typical diesel spray combustion, is unclear in Figure 4, because the amount of diesel fuel is too small at about 20 % of that of the full load.

Also, for both operating conditions, the concentrations of CH radicals increase, and then decrease in almost the same form after ignition; but in the case of the dual-fuel mode, it is reduced in a very short period of time. This is because the syngas, especially hydrogen with high laminar flame speed, within the diesel spray plume has contributed to the rapid burning of diesel fuel. In the previous studies of the diesel combustion process conducted by measuring chemiluminescence, CH radicals started to appear from the cool flame stage, and continued to exist during combustion (Costa *et al*., 2005). Therefore, the presence of CH radicals indicate that the burning of the hydrocarbon fuel is in progress; otherwise, it means that the hydrocarbon fuel is exhausted. OH radicals start to appear right after the appearance of CH radicals, and increase until the instance of the rapid drop of the CH radicals. When the CH radicals are almost depleted, the concentration of the OH radicals reaches the peak, and then gradually decreases. OH radicals form in the hot flame zone of hydrocarbons, and also are generated as an intermediate during the combustion process of hydrogen (Dec and Espey, 1998). The OH radicals after depletion of the CH radicals can be thought to have originated from the flame zone of hydrogen. In hydrogen combustion, the following elementary chemical reactions are the sources of OH radicals (Stylianidis *et al*., 2017; Curran, 2018):

$$O_2 + H = OH + O \quad (1)$$

$$H_2 + O = OH + H \quad (2)$$

$$H + O_2 (+ M) = HO_2 (+ M) \quad (3)$$

$$HO_2 + H = OH + OH \quad (4)$$

Figure 5 shows that when the flame propagates into the syngas region in the piston bowl after the rapid combustion of the diesel fuel, the amount of OH radicals maintains its peak value, due to the wide flame area in the piston bowl, while the temperature distributions in Figure 6 (a) show that the amount gradually decreases as the flame propagates into the squish area.

In the LSLB dual-fuel engine, the fuel-air mixture in the squish zone is almost composed of syngas and air, so the equivalence ratio of this mixture is extremely low, hence the flame propagation speed is low. Thus, it can expect that it takes significant time for the flame to arrive at the cylinder wall, which increases the time loss of the engine.

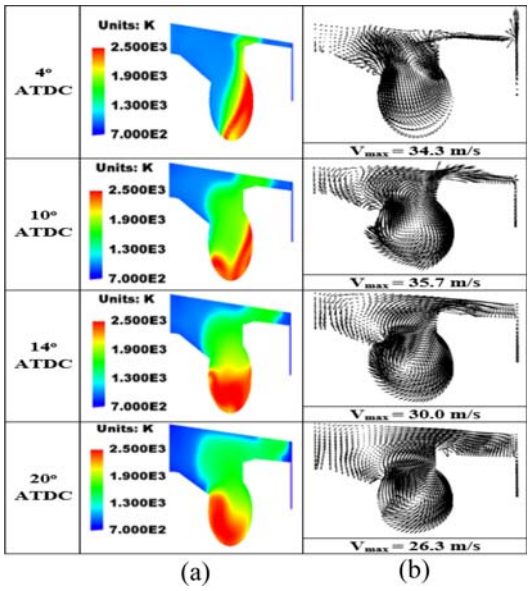

Figure 6. In-cylinder temperature distribution (a) and velocity vector field (b) at Syngas35, IMEP5 and 6G (center plane of the 72° sector mesh).

But it is apparent in Figure 4 and the sequential temperature distribution images of Figure 6 (a) that the flame arrives at the cylinder wall faster than expected from the HRRs. The reason for this phenomenon is the reverse squish flow, which is strongly formed in the squish region during the expansion process. The 14° ATDC velocity distribution in Figure 6 (b) shows that the maximum velocity of the reverse squish flow reaches 30 m/s, which is about 100 times greater than the laminar flame speed, which actually determines the speed at which the flame front moves in the squish area. In the squish zone, the fuel is almost all syngas. Thus, like the Spark Ignition (SI) engine, the flame propagation in the turbulent premixed mixture is the combustion mechanism. Since the mixture is extremely lean, and H_2 and CO in syngas have high auto-ignition temperature, flame quenching may occur early near the combustion chamber wall during the flame propagation, which causes high pollutants emission, such as CO and HC, which are represented in Figure 7.

In engine flow conditions, flame quenching is governed by a balance between the heat transfer to the preheat zone due to chemical heat release, and the heat loss from the preheat zone to the unburned mixture; in addition, disturbances from turbulence have significant influence on the transfer balance (Ansys Forte, 2017). The flame quenching model is used in the calculation which included in the Forte code. This model compares the inner layer thickness l_δ with the Kolmogorov length scale l_k, and assumes that flame quenching takes place under the condition of the following equation:

$$l_k < C_{m3}\, l_\delta \tag{5}$$

Where l_k is determined based on the turbulence model, and C_{m3} is a model constant with a typical value of 1.0.

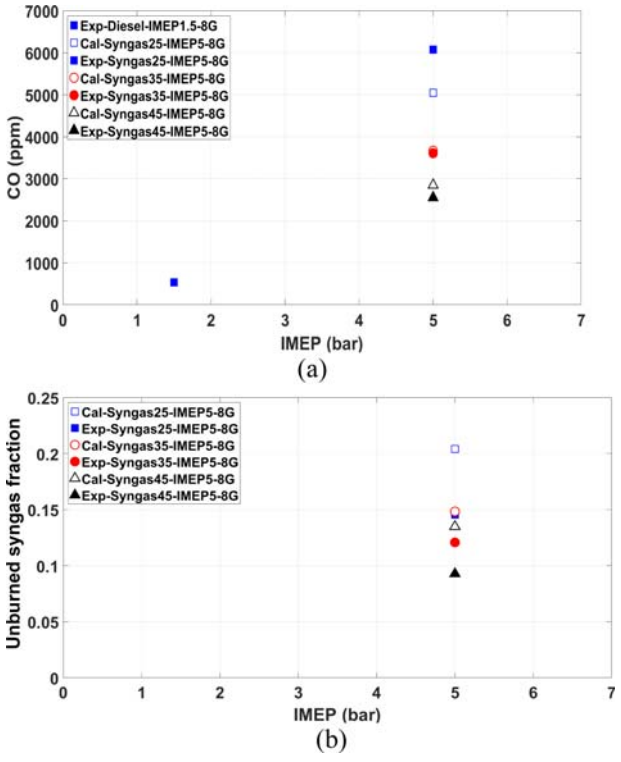

Figure 7. CO emission and unburned syngas fraction at IMEP 5 bar.

3.2. Effect of Syngas Composition on the Combustion Characteristics

Experiment and Calculation were performed for the LSLB dual-fuel engine to investigate the effect of syngas composition on the combustion characteristics. The overall calculation results for each syngas composition are in good agreement with the experimental results, and the trends are very similar.

As mentioned earlier, the syngas-only equivalence ratio is extremely low at about 0.235. The hydrogen concentration in the mixture is very low at 2.4 % and 3.7 % for syngas25 and syngas45, respectively. Considering the lower flammability limit of hydrogen is 1.2 % at the temperature of 90 °C and at the pressure of 4 bar (Liu and Zhang, 2014), it can be seen that the LSLB dual-fuel engine burns at very low hydrogen concentration.

Figure 8 represents the experimental and calculated pressure and HRR curves with respect to the syngas composition. In addition, Figure 9 compares the calculation results of the temperature distribution in the combustion chamber under syngas25 and syngas45 conditions.

In the early part of combustion, it can be seen that when the hydrogen concentration in the syngas is increased, the pressure rise after ignition occurs more steeply. This trend can be more clearly seen from the HRR curves. The trend is attributed to the fact that the syngas included in the spray plumes, particularly hydrogen, contributes to rapid burning of the diesel and syngas fuel in the early part of a dual-fuel mode combustion, due to its high flame speed.

The middle part of the combustion is due to the combustion of syngas in the region B+C1+W1; the piston bowl region except for the spray plume and the squish regions except for C2, the central part of the combustion chamber and W2, near the cylinder wall as remarked in Figure 10 (a). The pattern of the middle part combustion

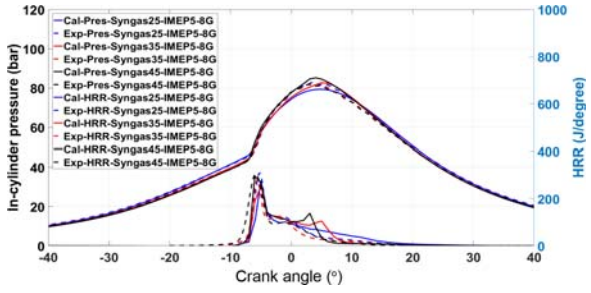

Figure 8. Comparison of experimental and numerical in-cylinder pressure and HRR for different syngas composition.

varies greatly depending on the syngas composition, as shown in the HRR curves of Figure 8.

When the hydrogen concentration is high, the syngas in the region B+C1+W1 is combusted in the vicinity of TDC; but when hydrogen concentration is low as in syngas25, flame propagation to the center region of the piston is delayed, which leads to an increase of time loss and unburned syngas emission.

In fact, the unburned syngas fraction of syngas25 increased significantly to 14.6 % in the experimental results, and showed a similar tendency in the calculated results, as shown in Figure 7.

It is considered that the flame speed is slow in the central region C1, due to the flow field in the combustion chamber. In the case of this engine, the squish area is large, thus negative pressure is generated in the squish area W1 during the expansion stroke of the piston, so that a strong reverse squish flow is generated in that direction, and the flow toward the central region C1 is relatively weak.

During the late combustion period of a normal combustion, the syngas in the central part of the combustion chamber, C2 and the outer squish region, W2 are mainly burned. However, in the case of syngas25 with a slow flame speed, the syngas in the C1 region is burned slowly, so that a portion that does not burn in the C1 and C2 regions occurs, which is the main source of the unburned syngas emission.

The temperature distributions in Figure 9 show that the combustion in the outer squish region, W1, has been little affected by the syngas composition.

This is due to the strong reverse squish flow, which is tens of times higher than the turbulent flame speed. In order to confirm this, the apparent flame speeds deduced from the temperature calculation results at the two points in Figure 10 (a) are obtained, and are shown in Figure 10 (b), which are 21.3 m/s for syngas45, and 10 % lower value for syngas25.

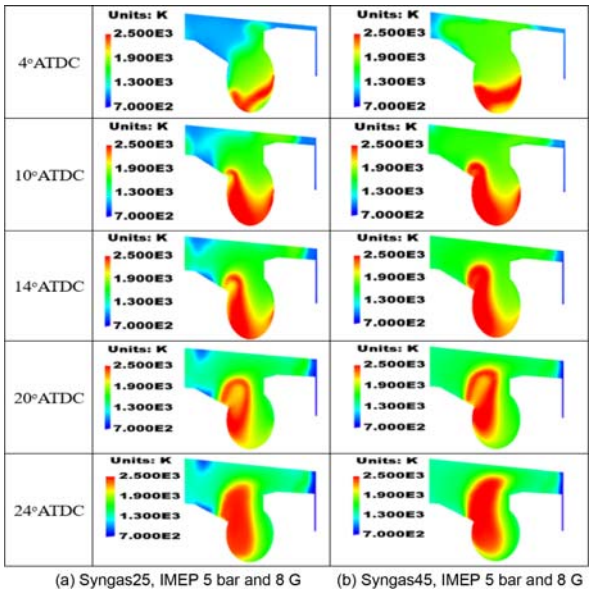

Figure 9. Comparison of the in-cylinder temperature distribution for different syngas composition (Center plane of the 72° sector mesh).

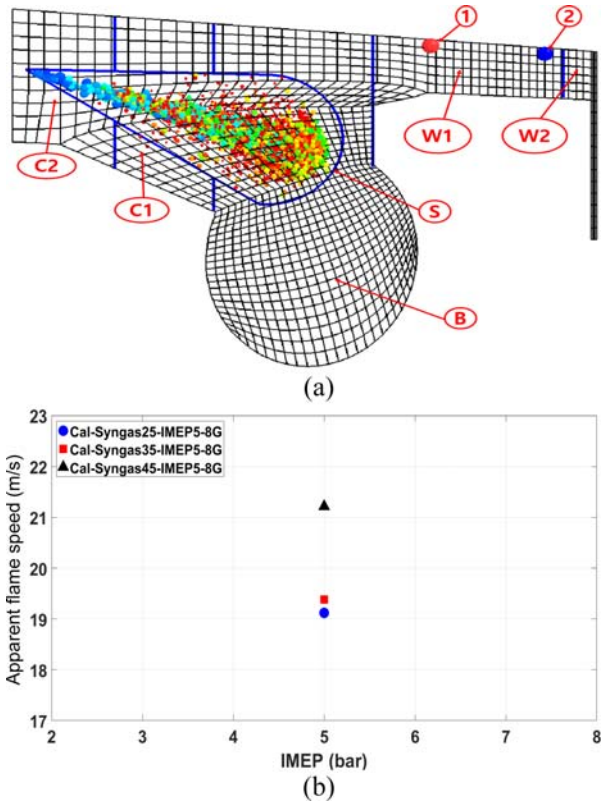

Figure 10. Area classification and temperature probe cells (a) and apparent flame speed between the cell ① and ② in the squish zone (b) with respect to the syngas composition.

Figure 11 shows the calculated peak and average temperatures in the combustion chamber according to the syngas composition and Figure 12 shows the NOx emission. The peak temperatures of syngas45 and syngas25 are 2,940 K and 2,810 K, respectively, which is a

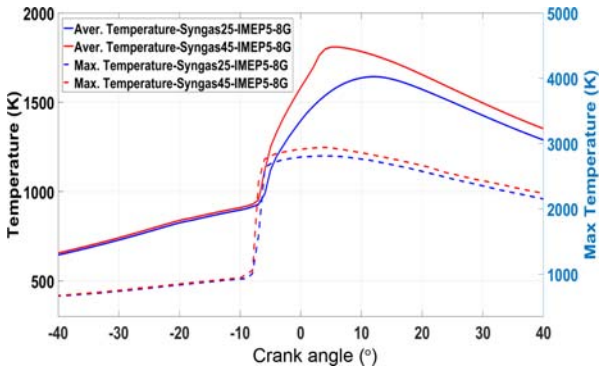

Figure 11. Average and Maximum temperature for different syngas composition.

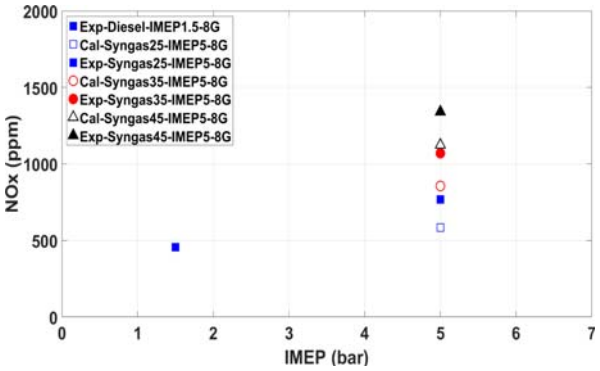

Figure 12. NOx emission with respect to the syngas composition at IMEP 5 bar.

130 K difference, but the average temperature shows a 55 K difference. Due to this temperature difference, the NOx emission of syngas 45 with high hydrogen concentration is about three times higher than the diesel-only mode, where the diesel fuel amount is similar. On the other hand, syngas25 is 1.6 times lower. The NOx concentration by calculation also shows a similar tendency, although there is a slight difference in the absolute value.

Considering that the load in the IMEP 5 bar dual-fuel mode operation was 3.3 times greater than that in the IMEP 1.5 bar diesel-only mode operation, the NOx concentration in syngas 45 increased in proportion to the load increase. However, in the case of syngas25, the increase is small. It can be seen that the increase of the hydrogen concentration has a great influence on the NOx increase.

4. CONCLUSION

In this study, the combustion characteristics of the LSLB dual-fuel engine using syngas-diesel as fuels were investigated through experiments and simulations. The main feature of this dual-fuel engine is that syngas has a low calorific value, and this syngas is burned under excessively lean conditions. To compensate this problem, the diesel injection amount is about 20 % of the full load, which is much larger than that of a conventional dual-fuel engine.

To simulate the combustion for the dual fuel engine, a new dual-fuel chemical kinetics set was used, which was constituted by merging two chemical kinetics sets: n-heptane (173 species), and Gri-mech 3.0 (53 species). The calculation results obtained by applying the merged chemical kinetics set are in good agreements with the experimental results from the viewpoint of combustion chamber pressure in a wide range of the dual-fuel mode.

This engine showed ignition timings that are the same for all dual-fuel mode operations that used the same injection timing, because auto-ignition is dominated by diesel, which is the source of ignition. After the ignition, most of the diesel fuel burned in premixed combustion mode, which can be computationally confirmed from the trace of CH radicals, because the diesel injection amount was small, at about 20 % of that of the full load.

After the combustion of the diesel fuel, the flame propagated into the syngas in the piston bowl, and then the flame proceeded toward the syngas of the squish zone. In this flame propagation stage, syngas composition, particularly hydrogen concentration, played an important role, since the flame propagation proceeded in the extremely lean syngas-air mixture condition. When the hydrogen concentration is high, as in syngas45, most of the syngas in the piston bowl and squish region, except near the cylinder wall, is combusted in the vicinity of TDC; but when hydrogen concentration is low, as in syngas25, flame propagation to the central region of the piston is delayed, which leads to an increase of time loss and unburned syngas emission. Due to the strong reverse squish flow, the flame arrival time at the cylinder wall through the squish area was not much affected by the syngas composition.

In conclusion, to improve the combustion efficiency and to reduce the unburned syngas fraction of the LSLB engine, optimization of the piston bowl shape and squish area should be performed, as well as optimizing the syngas composition.

ACKNOWLEDGEMENT–This work was supported by the National Research Council of Science and Technology (NST) grant by the Korean government (MSIT) (No.CAP-16-06-KIER).

REFERENCES

Abani, N., Kokjohn, S., Park, S. W., Bergin, M., Munnannur, A., Ning, W., Sun, Y. and Reitz, R. D. (2008). An improved spray model for reducing numerical parameter dependencies in diesel engine CFD simulations. *SAE Paper No*. 2008-01-0970.

Ansys Forte (2017). Forte Theory Manual. Release 18.2.

Azimov, U., Tomita, E., Kawahara, N. and Dol, S. S. (2012). Combustion characteristics of syngas and natural gas in micro-pilot ignited dual-fuel engine. *Int. J. Mechanical and Mechatronics Engineering* **6**, **12**, 2863–2870.

Beale, J. C. and Reitz, R. D. (1999). Modeling spray atomization with the Kelvin-Helmholtz/Rayleigh-Taylor hybrid model. *Atomization and Sprays* **9**, **6**, 623–650.

Bilcan, A. (2003). *Contribution to the Study of the Thermodynamic Cycle of Dual-fuel*. Ph. D. Dissertation. Nantes University. Nantes, France.

Bilcan, A., Le Corre, O., Tazerout, M., Ramesh, A. and Ganesan, S. (2001). Characterization of the LPG-diesel dual fuel combustion. *SAE Paper No*. 2001-28-0036.

Christodoulou, F. and Megaritis, A. (2014). The effect of reformer gas mixture on the performance and emissions of an HSDI diesel engine. *Int. J. Hydrogen Energy* **39**, **18**, 9798–9808.

Claudio, F., Cristian, C., Giulio, C., Marco, B. G., Stefania,

F., Federico, B., Alessandro, V. and Stefano, S. (2015). Numerical evaluation of the applicability of steady test bench swirl ratios to diesel engine dynamic conditions. *Energy Procedia*, **81**, 732–741.

Costa, M., Vaglieco, B. M. and Corcione, F. E. (2005). Radical species in the cool-flame regime of diesel combustion: A comparative numerical and experimental study. *Experiments in Fluids* **39**, **3**, 514–526.

Curran, H. J. (2018). Developing detailed chemical kinetic mechanisms for fuel combustion. *Proc. Combustion Institute* **37**, **1**, 57–81.

Dec, J. E. and Espey, C. (1998). Chemiluminescence imaging of autoignition in a DI diesel engine. *SAE Paper No*. 982685.

Elnajjar, E., Selim, M. Y. E. and Hamdan, M. O. (2013). Experimental study of dual fuel engine performance using variable LPG composition and engine parameters. *Energy Conversion and Management*, **76**, 32–42.

Smith, G. P., Golden, D. M., Frenklach, M., Moriarty, N. W., Eiteneer, B., Goldenberg, M., Bowman, C. T., Hanson, R. K., Song, S., Gardiner, W. C., Jr., Lissianski, V. V. and Qin, Z. (2018). http://combustion.berkeley.edu/gri-mech/version30/text30.html

Hiroyasu, H. and Masataka, A. (1990). Structures of fuel sprays in diesel engines. *SAE Trans*. **99**, **3**, 1050–1061.

Jamrozik, A., Tutak, W., Pyrc, M., Gruca, M. and Kočiško, M. (2018). Study on co-combustion of diesel fuel with oxygenated alcohols in a compression ignition dual-fuel engine. *Fuel*, **221**, 329–345.

Karim, G. A. (1991). An examination of some measures for improving the performance of gas fuelled diesel engines at light load. *SAE Trans*. **100**, **4**, 966–974.

Karim, G. A. and Moore, N. P. W. (1990). The production of hydrogen by the partial oxidation of methane in a dual fuel engine. *SAE Paper No*. 901501.

Karim, G. A. and Wierzba, I. (1992). Safety measures associated with the operation of engines on various alternative fuels. *Reliability Engineering & System Safety* **37**, **2**, 93–98.

Karim, G., Ito, K., Abraham, M. and Jensen, L. (1991). An examination of the role of formaldehyde in the ignition processes of a dual fuel engine. *SAE Trans*. **100**, **4**, 975–982.

Lata, D. B., Misra, A. and Medhekar, S. (2011). Investigations on the combustion parameters of a dual fuel diesel engine with hydrogen and LPG as secondary fuels. *Int. J. Hydrogen Energy* **36**, **21**, 13808–13819.

Li, Y., Li, H., Guo, H., Wang, H. and Yao, M. (2018). A numerical study on the chemical kinetics process during auto-ignition of n-heptane in a direct injection compression ignition engine. *Applied Energy*, **212**, 909–918.

Liang, L., Stevens, J. G. and Farrell, J. T. (2009). A dynamic multi-zone partitioning scheme for solving detailed chemical kinetics in reactive flow computations. *Combustion Science and Technology* **181**, **11**, 1345–1371.

Liang, W., Mével, R. and Law, C. K. (2018). Role of low-temperature chemistry in detonation of n-heptane/oxygen/diluent mixtures. *Combustion and Flame*, **193**, 463–470.

Liu, X. and Zhang, Q. (2014). Influence of initial pressure and temperature on flammability limits of hydrogen–air. *Int. J. Hydrogen Energy* **39**, **12**, 6774–6782.

Maghbouli, A., Saray, R. K., Shafee, S. and Ghafouri, J. (2013). Numerical study of combustion and emission characteristics of dual-fuel engines using 3D-CFD models coupled with chemical kinetics. *Fuel*, **106**, 98–105.

Maroteaux, F. (2017). Development of a two-part n-heptane oxidation mechanism for two stage combustion process in internal combustion engines. *Combustion and Flame*, **186**, 1–16.

Mcmillian, M. H. and Lawson, S. A. (2006). Experimental and modeling study of hydrogen/syngas production and particulate emissions from a natural gas-fueled partial oxidation engine. *Int. J. Hydrogen Energy* **31**, **7**, 847–860.

Sahoo, B. B., Sahoo, N. and Saha, U. K. (2009). Effect of engine parameters and type of gaseous fuel on the performance of dual-fuel gas diesel engines – A critical review. *Renewable and Sustainable Energy Reviews* **13**, **6-7**, 1151–1184.

Saxena, P. and Williams, F. A. (2006). Testing a small detailed chemical-kinetic mechanism for the combustion of hydrogen and carbon monoxide. *Combustion and Flame* **145**, **1-2**, 316–323.

Selim, M. Y. (2005). Effect of engine parameters and gaseous fuel type on the cyclic variability of dual fuel engines. *Fuel* **84**, **7-8**, 961–971.

Stylianidis, N., Azimov, U., Maheri, A., Tomita, E. and Kawahara, N. (2017). Chemical kinetics and CFD analysis of supercharged micro-pilot ignited dual-fuel engine combustion of syngas. *Fuel*, **203**, 591–606.

Talibi, M., Hellier, P., Balachandran, R. and Ladommatos, N. (2014). Effect of hydrogen-diesel fuel co-combustion on exhaust emissions with verification using an in–cylinder gas sampling technique. *Int. J. Hydrogen Energy* **39**, **27**, 15088–15102.

Tomita, E. (2007). Combustion characteristics and performance of supercharged pyrolysis gas engine with micro-pilot ignition. *Proc. 25th CIMAC World Cong. Combustion Engine Technology (CIMAC 2007)*, Vienna, Austria.

Wang, Y., Ge, H.-W. and Reitz, R. D. (2010). Validation of mesh- and timestep- independent spray models for multi-dimensional engine CFD simulation. *SAE Int. J. Fuels and Lubricants* **3**, **1**, 277–302.

Yang, B., Yao, M., Cheng, W. K., Li, Y., Zheng, Z. and Li, S. (2014). Experimental and numerical study on different dual-fuel combustion modes fuelled with gasoline and diesel. *Applied Energy*, **113**, 722–733.

Yetter, R. A., Dryer, F. L. and Rabitz, H. (1991). A comprehensive reaction mechanism for carbon monoxide/hydrogen/oxygen kinetics. *Combustion Science and Technology* **79**, **1-3**, 97–128.